

Communication

Role of N1-Domain, Linker, N2-Domain, and Latch in the Binding Activity and Stability of the Collagen-Binding Domain for the Collagen-Binding Protein Cbm from *Streptococcus mutans*

Akari Nishi ¹, Azumi Hirata ², Atsushi Mukaiyama ³ , Shun-ichi Tanaka ¹, Ryota Nomura ⁴, Kazuhiko Nakano ⁵ 
and Kazufumi Takano ^{1,*} 

¹ Department of Biomolecular Chemistry, Kyoto Prefectural University, Kyoto 606-8522, Japan

² Department of Anatomy and Cell Biology, Osaka Medical and Pharmaceutical University, Takatsuki 569-8686, Japan

³ Department of Bioscience and Biotechnology, Fukui Prefectural University, Fukui 910-1195, Japan

⁴ Department of Pediatric Dentistry, Graduate School of Biomedical and Health Sciences, Hiroshima University, Hiroshima 734-8553, Japan

⁵ Department of Pediatric Dentistry, Osaka University Graduate School of Dentistry, Suita 565-0871, Japan

* Correspondence: takano@kpu.ac.jp

Abstract: A special type of *Streptococcus mutans* expressing collagen-binding proteins (CBPs), Cnm, and Cbm, on the cell surface has been shown to be highly pathogenic. It is believed that *S. mutans* with CBPs that has entered the blood vessel attaches to collagen molecules exposed from the damaged blood vessel, inhibiting aggregation by platelets and increasing bleeding. Therefore, it is crucial to understand the molecular characteristic features of CBPs to protect against and cure *S. mutans*-related diseases. In this work, we highlighted the Cbm/collagen-binding domain (CBD) and examined its binding ability and thermal stability using its domain/region exchange variants in more detail. The CBD comprises the N1-domain, a linker, N2-domain, and a latch (N1–N2~), where the latch interacts with the N1-domain to form a β -sheet. The collagen-binding activity of the Cbm/CBD domain/region exchange variants was investigated using ELISA. Binding assays demonstrated that the N-domain_linker_N-domain composition is necessary for collagen binding as previously reported, newly that the latch is involved in binding through the β -sheet with the N1-domain when the N1-domain is present at the N-terminal position, and that the N2-domain is particularly important for collagen binding at both the N- and C-terminal positions. Thermal denaturation experiments newly revealed that the linker and latch bound to the N-domain contribute to N-domain stabilization but have no effect on the N-domain_linker_N-domain molecule, which contains two N-domains. It has also been shown that the N-terminal N2-domain destabilizes the N-domain_linker_N-domain structure. The results of this study will contribute to the rapid detection of CBP, development of CBP-targeted therapies, and application of CBPs to protein engineering using their collagen-binding ability.

Keywords: collagen-binding protein; Cbm; collagen-binding domain; *Streptococcus mutans*; ELISA; stability



Citation: Nishi, A.; Hirata, A.; Mukaiyama, A.; Tanaka, S.-i.; Nomura, R.; Nakano, K.; Takano, K. Role of N1-Domain, Linker, N2-Domain, and Latch in the Binding Activity and Stability of the Collagen-Binding Domain for the Collagen-Binding Protein Cbm from *Streptococcus mutans*. *Physchem* **2024**, *4*, 120–130. <https://doi.org/10.3390/physchem4020009>

Academic Editor: Chih-Ching Huang

Received: 2 February 2024

Revised: 21 March 2024

Accepted: 10 April 2024

Published: 12 April 2024



Copyright: © 2024 by the authors. Licensee MDPI, Basel, Switzerland. This article is an open access article distributed under the terms and conditions of the Creative Commons Attribution (CC BY) license (<https://creativecommons.org/licenses/by/4.0/>).

1. Introduction

Streptococcus mutans is a bacterium that lives in the human oral cavity and is a significant contributor to tooth decay [1–4]. Oral bacteria frequently enter blood vessels through bleeding from dental procedures, such as tooth extraction, scaling, or brushing [5–7], but are often eliminated by the immune system. It has long been known that oral bacteria that invade the blood vessels and evade the immune system can produce bacteremia [8–11]. Infective endocarditis may develop from bacteremia in patients with underlying cardiac disease [8,12,13]. Infective endocarditis is not a disease with a high incidence; however,

when it does occur, it is known to form platelets, fibrin, and bacterial masses called verrucae in the valve leaflets and endocardium, causing many complications. Thus, it is associated with a high mortality rate [8,14,15]. *Streptococcus oralis* is a known causative agent of infective endocarditis and is frequently detected in the heart valves and blood of patients with infective endocarditis. Among the oral *Streptococcus* species, *S. sanguinis* and *S. mitis* are the most common causes of subacute infective endocarditis, followed by *S. mutans* [16–18]. Although *S. mutans* has long been known as a causative agent of infective endocarditis, the details of its pathogenesis are not well understood [19,20].

Recently, PCR analysis revealed that more than 80% of heart valves diagnosed with infective endocarditis and removed were positive for *S. mutans*, and most of them tested positive for collagen-binding genes [21]. In cerebral hemorrhage, a known complication of infective endocarditis, collagen-binding protein (CBP)-positive *S. mutans* was detected in the dental plaques of patients during or after treatment for cerebral hemorrhage at a rate of approximately 40%. The presence of this organism in the oral cavity is thought to increase the risk of cerebral hemorrhage by approximately four times [22]. In addition, the effects of CBP-positive *S. mutans* on systemic diseases (such as ulcerative colitis, nonalcoholic steatohepatitis, and IgA nephropathy) have been reported [23]. Thus, specific *S. mutans* strains expressing CBPs are highly pathogenic. Moreover, CBP-positive *S. mutans* can adhere to type I collagen and vascular endothelial cells, which are major components of the heart; however, strains in which the gene encoding the collagen-binding domain (CBD) of CBP-positive *S. mutans* has been inactivated have been found to be unable to adhere to collagen and vascular endothelial cells [24]. Therefore, CBP-positive *S. mutans* is believed to adhere to exposed collagen molecules and vascular endothelial cells at the site of vascular injury through the binding ability of CBPs, thereby preventing aggregation by platelets and thus inhibiting hemostasis. This indicates the potential for the development of preventive and therapeutic methods against CBPs. To this end, it is important to understand the molecular properties of CBPs, especially the CBD, which has collagen-binding ability.

Cbm is a 57 kDa CBP expressed on the surface of *S. mutans* [25–27]. Cbm has high sequence homology to Cna, a CBP isolated from *S. aureus*; Ace, a CBP isolated from *Enterococcus faecalis*; and Cnm, a CBP isolated from *S. mutans* and Cbm [28–32]. A CBP is composed of a CBD, a B-repeat region, and a cell wall adhesion motif. The B-repeat region consists of two TTTE(K/A)P repeats and 19 TTTE(A/S/T)P repeats. Its role is speculated to be an axis for anchoring the CBD to the cell surface, extending and retracting from the cell wall, and supporting binding; however, its detailed function has not yet been elucidated [31,33]. The LPXTG motif plays a role in the presentation and immobilization of CBPs on the cell surface [34,35]. The CBD, with a molecular weight of 32 kDa, is the main collagen-binding region and consists of four regions on the N-terminal side: the N1-domain, linker, N2-domain, and latch [36]. In this study, we focused on the CBD of Cbm (Cbm/CBD), especially the constituent regions, the N1-domain, linker, N2-domain, and latch. The N1-domain, linker, N2-domain, and latch are denoted N1, –, N2, and ~, respectively. Thus, the full length of the CBD is N1–N2~.

Recently, we determined the crystal structure of the CBD in Cnm (Cnm/CBD) and presented a model structure for Cbm/CBD, as shown in Figure 1 [37]. N1_linker_N2 has a cyclic conformation to entrap collagen molecules, and the latch interworks with the β -strands of N1 to form the β -sheet structure. N1 and N2 possess analogous immunoglobulin folds [38,39]. The Cbm/CBD model structure was found to be similar to that of Cna/CBD in the Cna/CBD–synthetic collagen peptide complex [28]. This result suggests that the conformation of Cbm/CBD is comparable to the collagen-binding conformation of Cna/CBD. Therefore, it is likely that Cbm/CBD also binds to collagen by the Collagen Hug model proposed for Cna/CBD and Ace/CBD [28,29,40,41]. The Collagen Hug model is defined as follows: Y175 and F191 from the N2-domain form, stacking with Pro residues from collagen, the linker connecting the N1- and N2-domains interacts with collagen, and finally the latch on the C-terminal side of the N2-domain interacts with the N1-domain to form a β -sheet, resulting in the binding between CBD and collagen.

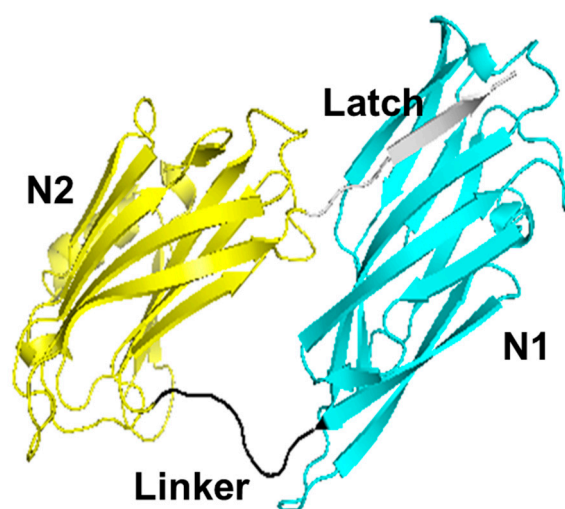


Figure 1. Model structure for Cbm/CBD.

In the previous work, furthermore, several domain/region exchange variants of Cbm/CBD were used to clarify the role of each region in collagen-binding activity and stability [37]. A collagen-binding assay showed that N1–N2~ and the latch-deletion variant (N1–N2) bound to collagen molecules with $K_D = 2.8$ and $28 \mu\text{M}$, but N1–N2 showed weaker binding, indicating that the latch is not essential for binding to collagen, but it does enhance binding [37]. The single-domain variants (N1 and N2) and linker-deleted variant (N1N2~) had no binding ability. On the contrary, the domain-swapped variant (N2–N1~) showed binding activity, implying that the two N-domains and the linker connecting them are required for collagen binding. Thermal unfolding measurements represented that N1–N2~ was slightly more stable than N1–N2, indicating that the latch bound to the N1-domain contributed to strengthening the overall structure of CBD, and that N2 was more stable than N1 [37]. In this study, we further constructed domain/region exchange variants and investigated the contribution of each region to the binding activity and stability in more detail. The results of this work supply fundamental insights into the development of CBP-targeted prophylaxis and therapy as well as the potential for a new approach to protein engineering: domain/region exchange variants.

The newly constructed variants are as follows. Since Cbm/CBD is the sequence of N1_linker_N2_latch (N1–N2~), to clarify the relationship between each N-domain and linker/latch, N1~ with N1_linker, ~N2 with linker_N2, ~N2~ with linker_N2_latch, and N2~ with N2_latch were designed. Each N-domain alone has no binding activity to collagen [20], so these variants were measured for thermal stability. Previously, we constructed the latch-deletion variant (N1–N2) and the domain-swapped variant (N2–N1~), and investigated the relationship between the latch and two N-domains connected by the linker, so this time we newly constructed N2–N1 with domain-swapped and latch-deleted variants, N1–N1~ and N2–N2~ with the two N-domains as the same N-domain, and N1–N1 and N2–N2 lacking the latch from them. Since the two N-domains connected by the linker (N1–N2~, N1–N2 and N2–N1~) showed binding activity [37], the binding activity of these variants was measured. Furthermore, the thermal stability of these variants was also investigated.

2. Materials and Methods

2.1. Expression and Purification

A pET-42a(+) vector with *Cbm* was previously constructed [22,42,43]. The cDNA of Cbm/CBD was previously re-cloned into pET-28a(+), and the resultant vector was used as a template to make the vectors for variant expression. The CBD and the variant regions (residue numbers) are listed in Table 1. *E. coli* BL21-CodonPlus(DE3)-RIL was transformed with the constructed plasmids. The *E. coli* organisms were grown at 37°C

up to OD₆₀₀ = 0.5, and IPTG at a final concentration of 1 mM induced protein expression and further culturing overnight at 18 °C. After the culturing, the cells were centrifuged and the precipitates were suspended in 50 mM Tris-HCl buffer and then ultrasonicated on ice. After centrifugation, the supernatants were subjected to a Ni-NTA affinity column and 16/60 Superdex 200 column. The proteins of interest were purified to a single band on SDS-PAGE.

Table 1. Residue numbers of CBD and the domain/region exchange variants of Cbm.

| Variants | Residue Numbers |
|-------------------------------|--------------------------------|
| Cbm/CBD (N1-N2~) ^a | 31-330 |
| N1 ^a | 31-163 |
| N1- | 31-171 |
| N2 ^a | 172-320 |
| -N2~ | 164-330 |
| N2~ | 172-330 |
| -N2 | 164-320 |
| N1-N2 ^a | 31-320 |
| N2-N1~ ^a | 172-320/164-171/31-163/321-330 |
| N2-N1 | 172-320/164-171/31-163 |
| N1-N1~ | 31-171/31-163/321-330 |
| N1-N1 | 31-171/31-163 |
| N2-N2~ | 172-320/164-330 |
| N2-N2 | 172-320/164-320 |

^a Previously constructed [37].

2.2. Collagen-Binding Assay

The collagen-binding activity was examined using ELISA, as described previously [37]. MaxiSorp plates (Nunc) were coated on each well with 1 µg of bovine dermis type I collagen (Nippi) in PBS and left overnight at 4 °C. The wells were then covered with 2% bovine serum albumin (BSA). After washing with 0.05% Tween in PBS, protein samples were subjected to the wells and kept for three hours at 37 °C. The wells were then rinsed with PBS-T and kept with anti-His-tag mAb-HRP-DirecT (MBL) diluted 1/10,000 with 0.1% BSA in PBS-T for one hour at 37 °C. Peroxidase substrate (TMB) and peroxide solution (H₂O₂) (Thermo SCIENTIFIC) were reacted for five minutes at room temperature as a chromogenic substrate solution. After that, the reaction was stopped by a 50 µL/well of 2 M H₂SO₄. After colorimetric reaction for 30 min, the absorption at 450 nm was measured. Binding curves were fitting the data to the following equation using SigmaPlot:

$$y = \frac{B_{max} \cdot x}{K_D + x} \tag{1}$$

where *y* represents the measured absorption at 450 nm, *B_{max}* represents the calculated maximal amplitude of the curve, *x* denotes the protein concentration, and *K_D* is the concentration that provides one-half of the shift between maximum and minimum readings. The results were obtained from the mean ± SD of triplicate experiments.

2.3. Thermal Denaturation

Thermal unfolding experiments were performed using CD at 218 nm, as described previously [37]. The protein concentration was 0.17 mg mL⁻¹ with 1 M GdnHCl in PBS at an optical path length of 2 mm. Scan rate was 1 °C min⁻¹. A nonlinear least-squares analysis was performed to fit the data to

$$y = \frac{(b_n + a_n[T]) + (b_u + a_u[T]) \exp\left[\left(\frac{\Delta H_m}{RT}\right)\left(\frac{T-T_m}{T_m}\right)\right]}{1 + \exp\left[\left(\frac{\Delta H_m}{RT}\right)\left(\frac{T-T_m}{T_m}\right)\right]} \tag{2}$$

where y is the observed CD signal at a given temperature $[T]$, b_n is the CD signal for the native state, b_u is the CD signal for the unfolded state, a_n is the slope of the pre-transition of the baseline, a_u is the slope of the post-transition of the baseline, ΔH_m is the enthalpy of unfolding at the transition midpoint temperature (T_m), and R is the gas constant. Curve fitting was conducted using SigmaPlot.

3. Results and Discussion

3.1. Collagen-Binding Activity of Cbm/CBD Domain/Region Exchange Variants

The binding ability of the Cbm/CBD domain/region exchange variants to type I collagen was examined using ELISA (Figure 2). The binding activity was estimated by calculating the K_D values (Table 2). As a result, the variants with two N-domains and a linker connecting them, except for N1–N1, showed micromolar-order binding activity. This is consistent with a previous study in which N1–N2~, N1–N2, and N2–N1~ had collagen-binding activity, but the linker-deletion variant (N1N2~) and single-domain variants (N1 and N2) had no binding ability (for N1–N1, see below) [38]. These results clearly show that the arrangement of the two N-domains and the linker connecting them—a ring structure encasing collagen consisting of N-domain_linker_N-domain—is required for collagen binding, as previously reported.

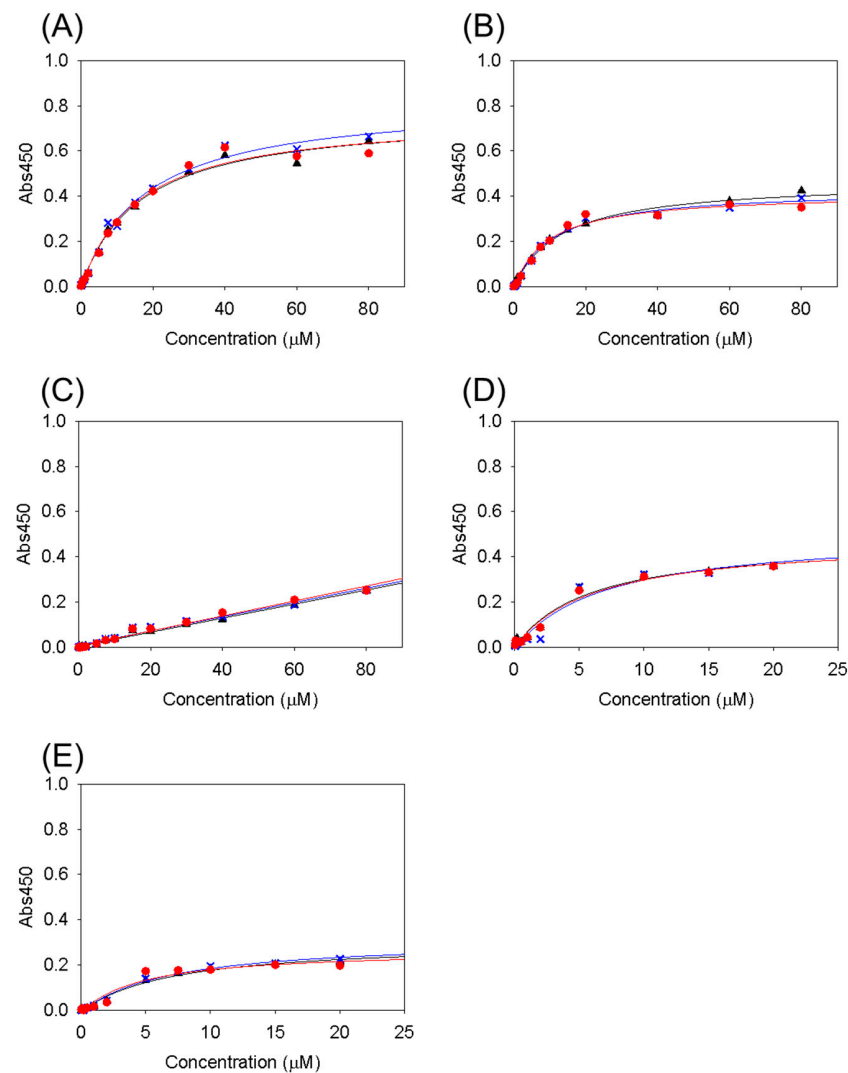


Figure 2. Binding curves measured using ELISA of (A) N2–N1, (B) N1–N1~, (C) N1–N1, (D) N2–N2~, and (E) N2–N2. The red circles, black triangles, and blue crosses and lines represent individual measurements. The lines are the best-fit curves according to Equation (1).

Table 2. K_D values for collagen binding of Cbm/CBD and its domain/region exchange variants measured using ELISA.

| Variants | K_D (μM) |
|-------------------------------|----------------------------|
| Cbm/CBD (N1–N2~) ^a | 2.8 ± 0.2 ^a |
| N1–N2 | 28 ± 6.5 ^a |
| N2–N1~ | 27 ± 2.9 ^a |
| N2–N1 | 16 ± 1.1 |
| N1–N1~ | 11 ± 2.1 |
| N1–N1 | ND |
| N2–N2~ | 6.2 ± 0.6 |
| N2–N2 | 6.2 ± 1.3 |

Errors represent the standard deviation (n = 3). ^a Data from [37].

N2–N2~ and N2–N2 showed similar binding activities ($K_D = 6.2 \mu\text{M}$). The latch in N2–N2~ cannot form the β -sheet with the N-terminal N2-domain, which does not have a latch interaction site in the β -sheet. Consequently, the latch cannot bind to the N2-domain at the N-terminal position, and N2–N2~ exhibited binding activity that was not significantly different from that of N2–N2. This is similar to the results for N2–N1~ and N2–N1, and the N2-domain at the N-terminal position and latch had no effect on the binding activity. In contrast, N1–N1~ was able to bind to collagen, whereas N1–N1 was not. This suggests that in N1–N1~, the N1-domain at the N-terminal position has a latch interaction site in the β -sheet; therefore, the latch interacts with the N1-domain at the N-terminal position to form a β -sheet. In other words, it was newly revealed that the latch was effective because of the presence of an N1-domain at the N-terminal position.

N2–N2~ and N2–N2 also showed stronger binding activity ($K_D = 6.2 \mu\text{M}$), closer to that ($K_D = 2.8 \mu\text{M}$) of Cbm/CBD (N1–N2~) than N2–N1~, N1–N2, and N2–N1 ($K_D = 27, 28$ and $16 \mu\text{M}$, respectively). These results indicate that the N2-domain contributes to collagen binding, whether located at the N-terminus or the C-terminus, and that the presence of two N2-domains further strengthens the binding. This suggests that the specific interaction of proline residues in collagen with Y175 and F191 in the N2-domain, as inferred from the structure, may be important [37]. Collagen has a triple-helical structure with glycine and proline residues repeating every three residues [44–46], and the N2-domain in the CBD binds and wraps around this collagen triple-helix structure through proline residues [28]. Therefore, it was newly shown that the N2-domain that interacts with collagen can be present at either the N- or C-terminus, and two N2-domains further enhance the binding force. In contrast, N1–N1, which lacks the N2-domain, could not bind to collagen. However, as mentioned above, the presence of the latch and N1-domain at the N-terminus allows for binding to collagen.

These results indicate that for the CBD to bind to collagen, in addition to the N-domain_linker_N-domain configuration, it requires the N2-domain that interacts with collagen (N1–N2, N2–N1~, and N2–N1), or both the N1-domain at the N-terminus and the latch that interacts with it to form a β -sheet (N1–N1~). The binding activity is enhanced when N2 and N1 at the N-terminus and latch are combined (N1–N2~) and when there are two N2-domains (N2–N2 and N2–N2~). On the other hand, the N-terminal N2-domain does not have a latch-binding site, so even if the latch is present (N2–N2~), it has no effect on binding. Thus, if we can design a β -sheet-forming site with a latch in the N2-domain that maintains the collagen-binding site, we may be able to construct a modified CBD with a higher binding capacity than Cbm/CBD (N1–N2~), N2–N2, and N2–N2~. Furthermore, these findings strongly support that Cbm/CBD is bound to collagen by the Collagen Hug model. The N2-domain that interacts with proline residues present abundantly in collagen, the linker that connects the two N-domains to form a ring structure to encase collagen, and the latch that forms the β -sheet with the N1-domain to hold collagen firmly in place are critical for collagen binding.

In this work, bovine type I collagen was used. The amino acid sequence homology between bovine and human type I collagen is over 90% [47,48]. However, to better understand the relationship between human diseases and Cbm/CBD, experiments using human collagen are required, and this is a future challenge.

3.2. Thermal Stability of Cbm/CBD Domain/Region Exchange Variants

To obtain the stability of each domain/region of the CBD, thermal unfoldings of Cbm/CBD domain/region exchange variants were examined using CD (Figure 3). Previously, the thermal unfolding curve of Cbm/CBD (N1–N2~) provided a single-step unfolding with a T_m value of 57.6 °C, resulting from predominantly N2-domain denaturation. Furthermore, the N2-domain was found to be more stable than the N1-domain [37].

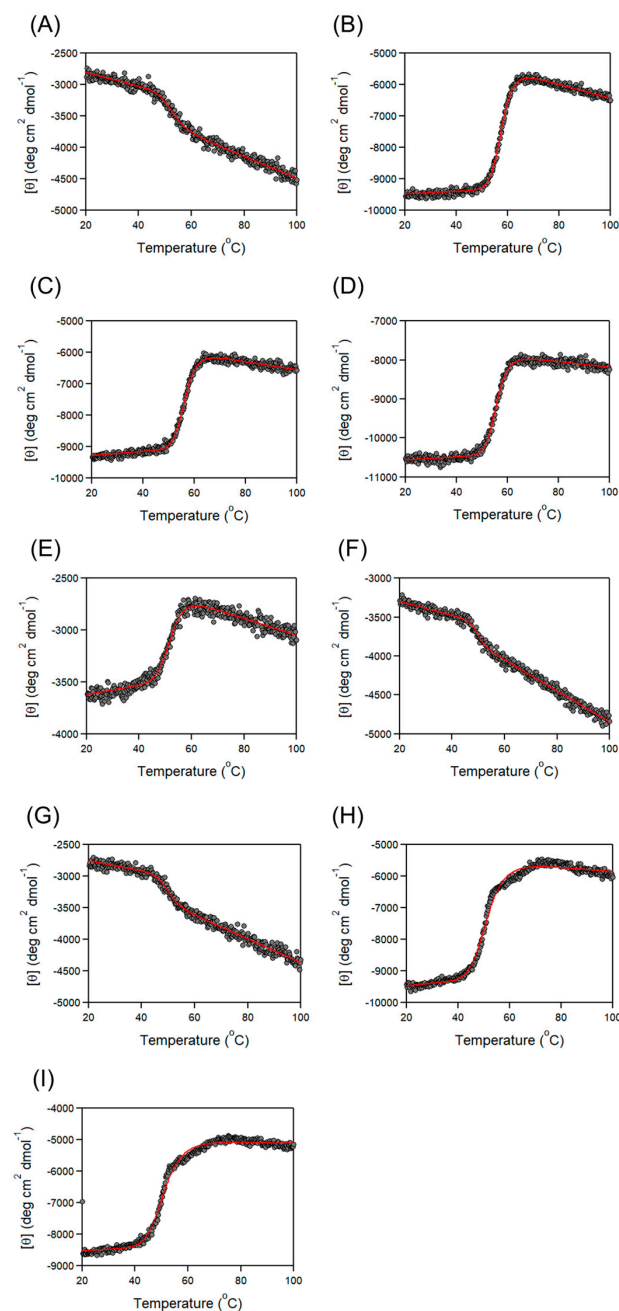


Figure 3. Thermal denaturation curves of (A) N1-, (B) -N2~, (C) N2~, (D) -N2~, (E) N2-N1, (F) N1-N1~, (G) N1-N1, (H) N2-N2~, and (I) N2-N2. The red lines are the best-fit curves according to Equation (2).

In this study, we first examined the effect of adding a linker and/or latch to one N-domain on the stability (Table 3). N1- (T_m : 52.4 °C) was slightly more stable than N1 (T_m : 50.7 °C). Similarly, -N2 (T_m : 55.6 °C) and N2~ (T_m : 56.3 °C) were also more stable than N2 (T_m : 54.2 °C). Moreover, -N2~ (T_m : 57.6 °C) showed higher stability. These results indicate that the linkers and latches bound to the N-domain contribute to the stabilization of the N-domain, which is a novel finding. In general, when an amino acid sequence added to a protein interacts with its protein, the protein is stabilized [49–51]. Thus, the linkers and latches that bind to the N1- and N2-domains are likely to interact in some way with the N1- and N2-domains. The interactions described here are different from the interaction between the latch and the N1-domain in the overall CBD structure due to the β -sheet formation. On the other hand, adding a latch to an N-domain_linker_N-domain structure with two N-domains, as in the comparison of N2-N1~ (T_m : 51.9 °C) and N2-N1 (T_m : 52.1 °C), N1-N1~ (T_m : 49.4 °C) and N1-N1 (T_m : 49.5 °C), and N2-N2~ (T_m : 51.2 °C) and N2-N2 (T_m : 50.8 °C), had little effect on stability. This indicates that even if a few polypeptide chain residues are added to one domain of a protein with two domains, its stabilizing effect may not be clearly visible.

Table 3. T_m values of Cbm/CBD and its domain/region exchange variants measured by CD.

| Variants | T_m (°C) |
|-------------------------------|-------------------------|
| Cbm/CBD (N1-N2~) ^a | 57.6 ± 0.1 ^a |
| N1 | 50.7 ± 0.3 ^a |
| N1- | 52.4 ± 0.4 |
| N2 | 54.2 ± 0.1 ^a |
| -N2~ | 57.6 ± 0.1 |
| N2~ | 56.3 ± 0.1 |
| -N2 | 55.6 ± 0.1 |
| N1-N2 | 55.2 ± 0.1 ^a |
| N2-N1~ | 51.9 ± 0.1 ^a |
| N2-N1 | 52.1 ± 0.2 |
| N1-N1~ | 49.4 ± 0.3 |
| N1-N1 | 49.5 ± 0.4 |
| N2-N2~ | 51.2 ± 0.1 |
| N2-N2 | 50.8 ± 0.2 |

Errors represent the ones from a nonlinear least-squares fit using Equation (2). ^a Data from [37].

Next, we investigated the positional dependence of the N2-domain. For the N-domain_linker_N-domain structure with the N2-domain at the C-terminus (N1-N2~ and N1-N2) and the variants with one N2-domain (N2, -N2~, N2~ and -N2), the T_m values were above 54 °C. In contrast, for the N-domain_linker_N-domain structure with the N2-domain at the N-terminus (N2-N1~, N2-N1, N2-N2~ and N2-N2), the T_m values were lower. The reason for this may be that the N-domain_linker_N-domain structure is unstable when an N2-domain is present at the N-terminus, or the addition of the linker to the N2-domain makes it unstable. Further validation using N2- with an N2_linker is required to clarify this.

3.3. Characteristics of Cbm/CBD Domain/Region Exchange Variants

The collagen-binding assays and heat denaturation experiments of Cbm/CBD domain/region exchange variants revealed the characteristics of each variant. These characteristics of the CBP's collagen-binding ability in protein engineering applications will now be discussed. Cbm/CBD (N1-N2~) was superior in both binding and stability. On the other hand, N1-N2, N2-N1~, N2-N1, and N1-N1~ showed reduced binding activity, but were still able to bind to collagen. This is useful for weakly binding to collagen and removing the CBD from collagen as easily as possible. N2-N2~ and N2-N2 with two N2-domains showed similar binding activity to N1-N2~ but lower stability than N1-N2~. In these cases, it may be possible to tune the binding capacity using heat.

4. Conclusions

In the present study, to comprehend the binding mechanism of Cbm/CBD to collagen and the structural properties of Cbm/CBD, we performed binding assays and stability measurements of the domain/region exchange variants of the CBD. Binding assays using domain/region exchange variants indicated that the N-domain_linker_N-domain arrangement is required for collagen binding, newly suggesting that the presence of an N1-domain at the N-terminus makes latching effective, and that the N2-domain is particularly important for collagen binding. Stability experiments newly revealed that the linker and latch attached to the N-domain contributed to the stabilization of the N-domain, whereas the N-domain_linker_N-domain structure with two N-domains had no effect. It was also shown that the presence of the N2-domain at the N-terminus destabilizes the N-domain_linker_N-domain structure.

Author Contributions: Conceptualization, A.H. and K.T.; Methodology, A.H., A.M. and S.-i.T.; Investigation, A.N.; Resources, R.N. and K.N.; Writing—Original Draft Preparation, K.T.; Writing—Review and Editing, A.N., A.H., A.M., S.-i.T., R.N., K.N. and K.T.; Supervision, K.N. and K.T.; Project administration, A.H. and S.-i.T.; Funding acquisition, A.H., S.-i.T. and R.N. All authors have read and agreed to the published version of the manuscript.

Funding: This study was supported by JSPS KAKENHI Grant Number JP15K15749, JP18K09735, JP22K10233, JP21K05386.

Data Availability Statement: The data that support the findings of this study are available from the corresponding author upon reasonable request.

Conflicts of Interest: The authors declare no conflicts of interest.

References

1. Shklair, I.L.; Keene, H.J.; Simonson, L.G. Distribution and frequency of *Streptococcus mutans* in caries-active individuals. *J. Dent. Res.* **1972**, *51*, 882. [[CrossRef](#)] [[PubMed](#)]
2. Hamada, S.; Slade, H.D. Biology, immunology, and cariogenicity of *Streptococcus mutans*. *Microbiol. Rev.* **1980**, *44*, 331–384. [[CrossRef](#)] [[PubMed](#)]
3. Lemos, J.A.; Palmer, S.R.; Zeng, L.; Wen, Z.T.; Kajfasz, J.K.; Freires, I.A.; Abranches, J.; Brady, L.J. The Biology of *Streptococcus mutans*. *Microbiol. Spectr.* **2019**, *7*, 10.1128. [[CrossRef](#)] [[PubMed](#)]
4. Merritt, J.; Qi, F. The mutacins of *Streptococcus mutans*: Regulation and ecology. *Mol. Oral. Microbiol.* **2012**, *27*, 57–69. [[CrossRef](#)] [[PubMed](#)]
5. Debelian, G.J.; Olsen, I.; Tronstad, L. Systemic diseases caused by oral microorganisms. *Endod. Dent. Traumatol.* **1994**, *10*, 57–65. [[CrossRef](#)]
6. Roberts, G.J.; Lucas, V.S.; Omar, J. Bacterial endocarditis and orthodontics. *J. R. Coll. Surg. Edinb.* **2000**, *45*, 141–145. [[PubMed](#)]
7. Inaba, H.; Amano, A. Roles of oral bacteria in cardiovascular diseases—From molecular mechanisms to clinical cases: Implication of periodontal diseases in development of systemic diseases. *J. Pharmacol. Sci.* **2010**, *113*, 103–109. [[CrossRef](#)] [[PubMed](#)]
8. Seymour, R.A.; Lowry, R.; Whitworth, J.M.; Martin, M.V. Infective endocarditis, dentistry and antibiotic prophylaxis; time for a rethink? *Br. Dent. J.* **2000**, *189*, 610–616. [[CrossRef](#)] [[PubMed](#)]
9. Iwai, T. Periodontal bacteremia and various vascular diseases. *J. Periodontal. Res.* **2009**, *44*, 689–694. [[CrossRef](#)]
10. Hirschfeld, J.; Kawai, T. Oral inflammation and bacteremia: Implications for chronic and acute systemic diseases involving major organs. *Cardiovasc. Hematol. Disord. Drug. Targets* **2015**, *15*, 70–84. [[CrossRef](#)]
11. Parahitiyawa, N.B.; Jin, L.J.; Leung, W.K.; Yam, W.C.; Samaranyake, L.P. Microbiology of odontogenic bacteremia: Beyond endocarditis. *Clin. Microbiol. Rev.* **2009**, *22*, 46–64. [[CrossRef](#)] [[PubMed](#)]
12. Roberts, G.J.; Gardner, P.; Simmons, N.A. Optimum sampling time for detection of dental bacteraemia in children. *Int. J. Cardiol.* **1992**, *35*, 311–315. [[CrossRef](#)] [[PubMed](#)]
13. Crawford, M.H.; Durack, D.T. Clinical presentation of infective endocarditis. *Cardiol. Clin.* **2003**, *21*, 159–166. [[CrossRef](#)] [[PubMed](#)]
14. Bayer, A.S.; Bolger, A.F.; Taubert, K.A.; Wilson, W.; Steckelberg, J.; Karchmer, A.W.; Levison, M.; Chambers, H.F.; Dajani, A.S.; Gewitz, M.H.; et al. Diagnosis and management of infective endocarditis and its complications. *Circulation* **1998**, *98*, 2936–2948. [[CrossRef](#)] [[PubMed](#)]
15. Thiene, G.; Basso, C. Pathology and pathogenesis of infective endocarditis in native heart valves. *Cardiovasc. Pathol.* **2006**, *15*, 256–263. [[CrossRef](#)] [[PubMed](#)]
16. Nakatani, S.; Mitsutake, K.; Ohara, T.; Kokubo, Y.; Yamamoto, H.; Hanai, S. CADRE Investigators: Recent picture of infective endocarditis in Japan—lessons from Cardiac Disease Registration (CADRE-IE). *Circ. J.* **2013**, *77*, 1558–1564. [[CrossRef](#)] [[PubMed](#)]

17. Nakano, K.; Nomura, R.; Ooshima, T. *Streptococcus mutans* and cardiovascular diseases. *Jpn. Dent. Sci. Rev.* **2008**, *44*, 29–37. [[CrossRef](#)]
18. Knox, K.W.; Hunter, N. The role of oral bacteria in the pathogenesis of infective endocarditis. *Aust. Dent. J.* **1991**, *36*, 286–292. [[CrossRef](#)]
19. McGhie, D.; Hutchison, J.G.; Nye, F.; Ball, A.P. Infective endocarditis caused by *Streptococcus mutans*. *Br. Heart J.* **1977**, *39*, 456–458. [[CrossRef](#)]
20. Vose, J.M.; Smith, P.W.; Henry, M.; Colan, D. Recurrent *Streptococcus mutans* endocarditis. *Am. J. Med.* **1987**, *23*, 630–632. [[CrossRef](#)]
21. Nomura, R.; Naka, S.; Nemoto, H.; Inagaki, S.; Taniguchi, K.; Ooshima, T.; Nakano, K. Potential involvement of collagen-binding proteins of *Streptococcus mutans* in infective endocarditis. *Oral Dis.* **2013**, *19*, 387–393. [[CrossRef](#)] [[PubMed](#)]
22. Nakano, K.; Hokamura, K.; Taniguchi, N.; Wada, K.; Kudo, C.; Nomura, R.; Kojima, A.; Naka, S.; Muranaka, Y.; Thura, M.; et al. The collagen-binding protein of *Streptococcus mutans* is involved in haemorrhagic stroke. *Nat. Commun.* **2011**, *2*, 485. [[CrossRef](#)] [[PubMed](#)]
23. Tonomura, S.; Ihara, M.; Kawano, T.; Tanaka, T.; Okuno, Y.; Saito, S.; Friedland, R.P.; Kuriyama, N.; Nomura, R.; Watanabe, Y.; et al. Intracerebral hemorrhage and deep microbleeds associated with cnm-positive *Streptococcus mutans*; a hospital cohort study. *Sci. Rep.* **2016**, *5*, 20074. [[CrossRef](#)] [[PubMed](#)]
24. Nomura, R.; Ogaya, Y.; Nakano, K. Contribution of the collagen-binding proteins of *Streptococcus mutans* to bacterial colonization of inflamed dental pulp. *PLoS ONE* **2016**, *11*, e0159613. [[CrossRef](#)] [[PubMed](#)]
25. Sato, Y.; Okamoto, K.; Kagami, A.; Yamamoto, Y.; Igarashi, T.; Kizaki, H. *Streptococcus mutans* strains harboring collagen-binding adhesin. *J. Dent. Res.* **2004**, *83*, 534–539. [[CrossRef](#)] [[PubMed](#)]
26. Nomura, R.; Nakano, K.; Naka, S.; Nemoto, H.; Masuda, K.; Lapirattanakul, J.; Alaluusua, S.; Matsumoto, M.; Kawabata, S.; Ooshima, T. Identification and characterization of a collagen-binding protein, Cbm, in *Streptococcus mutans*. *Mol. Oral Microbiol.* **2012**, *27*, 308–323. [[CrossRef](#)]
27. Avilés-Reyes, A.; Miller, J.H.; Lemos, J.A.; Abranches, J. Collagen-binding proteins of *Streptococcus mutans* and related streptococci. *Mol. Oral Microbiol.* **2017**, *32*, 89–106. [[CrossRef](#)]
28. Zong, Y.; Xu, Y.; Liang, X.; Keene, D.R.; Höök, A.; Gurusiddappa, S.; Höök, M.; Narayana, S.V. A ‘Collagen Hug’ model for *Staphylococcus aureus* CNA binding to collagen. *EMBO J.* **2005**, *24*, 4224–4236. [[CrossRef](#)] [[PubMed](#)]
29. Liu, Q.; Ponnuraj, K.; Xu, Y.; Ganesh, V.K.; Sillanpää, J.; Murray, B.E.; Narayana, S.V.; Höök, M. The *Enterococcus faecalis* MSCRAMM ACE binds its ligand by the Collagen Hug model. *J. Biol. Chem.* **2007**, *282*, 19629–19637. [[CrossRef](#)]
30. Herman-Bausier, P.; Valotteau, C.; Pietrocola, G.; Rindi, S.; Alsteens, D.; Foster, T.J.; Speziale, P.; Dufrêne, Y.F. Mechanical strength and inhibition of the *Staphylococcus aureus* collagen-binding protein Cna. *mBio* **2016**, *25*, e01529-16. [[CrossRef](#)]
31. Valotteau, C.; Prystopiuk, V.; Pietrocola, G.; Rindi, S.; Peterle, D.; De Filippis, V.; Foster, T.J.; Speziale, P.; Dufrêne, Y.F. Single-cell and single-molecule analysis unravels the multifunctionality of the *Staphylococcus aureus* collagen-binding protein Cna. *ACS Nano* **2017**, *11*, 2160–2170. [[CrossRef](#)] [[PubMed](#)]
32. Singh, K.V.; Nallapareddy, S.R.; Sillanpää, J.; Murray, B.E. Importance of the collagen adhesin ace in pathogenesis and protection against *Enterococcus faecalis* experimental endocarditis. *PLoS Pathog.* **2010**, *8*, e1000716.
33. Igarashi, T.; Asaga, E.; Goto, N. The sortase of *Streptococcus mutans* mediates cell wall anchoring of a surface protein antigen. *Oral Microbiol. Immunol.* **2003**, *18*, 266–269. [[CrossRef](#)] [[PubMed](#)]
34. Boekhorst, J.; de Been, M.W.; Kleerebezem, M.; Siezen, R.J. Genome-wide detection and analysis of cell wall-bound proteins with LPxTG-like sorting motifs. *J. Bacteriol.* **2005**, *187*, 4928–4934. [[CrossRef](#)] [[PubMed](#)]
35. Freund, C.; Schwarzer, D. Engineered sortases in peptide and protein chemistry. *Chembiochem* **2021**, *16*, 1347–1356. [[CrossRef](#)] [[PubMed](#)]
36. Arora, S.; Gordon, J.; Hook, M. Collagen binding proteins of gram-positive pathogens. *Front Microbiol.* **2021**, *5*, 628798. [[CrossRef](#)] [[PubMed](#)]
37. Nishi, A.; Matsui, H.; Hirata, A.; Mukaiyama, A.; Tanaka, S.-i.; Yoshizawa, T.; Matsumura, H.; Nomura, R.; Nakano, K.; Takano, K. Structure, stability and binding properties of collagen-binding domains from *Streptococcus mutans*. *Chemistry* **2023**, *5*, 1911–1920. [[CrossRef](#)]
38. Bork, P.; Holm, L.; Sander, C. The immunoglobulin fold. Structural classification, sequence patterns and common core. *J. Mol. Biol.* **1994**, *242*, 309–320. [[CrossRef](#)] [[PubMed](#)]
39. Mirny, L.A.; Shakhnovich, E.I. Universally conserved positions in protein folds: Reading evolutionary signals about stability, folding kinetics and function. *J. Mol. Biol.* **1999**, *291*, 177–196. [[CrossRef](#)]
40. Madani, A.; Garakani, K.; Mofrad, M.R.K. Molecular mechanics of *Staphylococcus aureus* adhesin, CNA, and the inhibition of bacterial adhesion by stretching collagen. *PLoS ONE* **2017**, *12*, e0179601. [[CrossRef](#)]
41. Foster, T.J. The MSCRAMM family of cell-wall-anchored surface proteins of gram-positive cocci. *Trends Microbiol.* **2019**, *27*, 927–941. [[CrossRef](#)] [[PubMed](#)]
42. Matsumoto-Nakano, M.; Fujita, K.; Ooshima, T. Comparison of glucan-binding proteins in cariogenicity of *Streptococcus mutans*. *Oral Microbiol. Immunol.* **2007**, *22*, 30–35. [[CrossRef](#)] [[PubMed](#)]
43. Nomura, R.; Otsugu, M.; Naka, S.; Teramoto, N.; Kojima, A.; Muranaka, Y.; Matsumoto-Nakano, M.; Ooshima, T.; Nakano, K. Contribution of the interaction of *Streptococcus mutans* serotype *k* strains with fibrinogen to the pathogenicity of infective endocarditis. *Infect. Immun.* **2014**, *82*, 5223–5234. [[CrossRef](#)] [[PubMed](#)]

44. Brodsky, B.; Ramshaw, J.A. The collagen triple-helix structure. *Matrix Biol.* **1997**, *15*, 545–554. [[CrossRef](#)] [[PubMed](#)]
45. Bhattacharjee, A.; Bansal, M. Collagen structure: The Madras triple helix and the current scenario. *IUBMB Life* **2005**, *57*, 161–172. [[CrossRef](#)] [[PubMed](#)]
46. Amirrah, I.N.; Lokanathan, Y.; Zulkiflee, I.; Wee, M.F.M.R.; Motta, A.; Fauzi, M.B. A Comprehensive review on collagen type I development of biomaterials for tissue engineering: From biosynthesis to bioscaffold. *Biomedicines* **2022**, *10*, 2307. [[CrossRef](#)] [[PubMed](#)]
47. Gallo, N.; Natali, M.L.; Sannino, A.; Salvatore, L. An overview of the use of equine collagen as emerging material for biomedical applications. *J. Funct. Biomater.* **2020**, *11*, 79. [[CrossRef](#)] [[PubMed](#)]
48. Naomi, R.; Ridzuan, P.M.; Bahari, H. Current insights into collagen type I. *Polymers* **2021**, *13*, 2642. [[CrossRef](#)] [[PubMed](#)]
49. Takano, K.; Okamoto, T.; Okada, J.; Tanaka, S.; Angkawidjaja, C.; Koga, Y.; Kanaya, S. Stabilization by fusion to the C-terminus of hyperthermophile *Sulfolobus tokodaii* RNase HI: A possibility of protein stabilization tag. *PLoS ONE* **2011**, *19*, e16226. [[CrossRef](#)]
50. Matsuura, T.; Miyai, K.; Trakulnaleamsai, S.; Yomo, T.; Shima, Y.; Miki, S.; Yamamoto, K.; Urabe, I. Evolutionary molecular engineering by random elongation mutagenesis. *Nat. Biotechnol.* **1999**, *17*, 58–61. [[CrossRef](#)]
51. Wang, M.; Feng, Y.; Yao, H.; Wang, J. Importance of the C-terminal loop L137-S141 for the folding and folding stability of staphylococcal nuclease. *Biochemistry* **2010**, *49*, 4318–4326. [[CrossRef](#)] [[PubMed](#)]

Disclaimer/Publisher’s Note: The statements, opinions and data contained in all publications are solely those of the individual author(s) and contributor(s) and not of MDPI and/or the editor(s). MDPI and/or the editor(s) disclaim responsibility for any injury to people or property resulting from any ideas, methods, instructions or products referred to in the content.